Nearest neighbor exchange in Co- and Mn-doped ZnO

Thomas Chanier, M. Sargolzaei, I. Opahle, R. Hayn, K. Koepernik

Nearest neighbor exchange in Co- and Mn-doped ZnO

T. Chanier,[1] M. Sargolzaei,[2] I. Opahle,[2] R. Hayn,[1] and K. Koepernik[2]

[1]*Laboratoire Matériaux et Microélectronique de Provence, Faculté St. Jérôme, Case 142, F-13397 Marseille Cedex 20, France*

[2]*Leibniz-Institut für Festkörper- und Werkstoffforschung Dresden, P.O.Box 270116, D-01171 Dresden, Germany*

(Dated: November 2, 2005)

We calculate the magnetic interactions between two nearest neighbor substitutional magnetic ions (Co or Mn) in ZnO by means of density functional theory and compare it with the available experimental data. Using the local spin density approximation we find a coexistence of ferro- and antiferromagnetic couplings for ZnO:Co, in contrast to experiment. For ZnO:Mn both couplings are antiferromagnetic but deviate quantitatively from measurement. That points to the necessity to account better for the strong electron correlation at the transition ion site which we have done by applying the LSDA+U method. We show that we have to distinguish two different nearest neighbor exchange integrals for the two systems in question which are all antiferromagnetic with values between -1.0 and -2.0 meV in reasonable agreement with experiment.

PACS numbers: 75.50.Pp,71.20.Nr,71.23.An,71.55.Gs

I. INTRODUCTION

The manipulation of the electronic spin for information processing gives rise to many advantages and would open the way to new applications. This field of spintronics has need of a semiconducting, ferromagnetic material at room temperature. In that respect, several observations of room temperature ferromagnetism in ZnO:Co[1,2] or ZnO:Mn[3] had been reported. These experimental findings were partly based on theoretical predictions using density functional calculations in the local spin density approximation (LSDA).[3,4] However, they are not at all confirmed. Whereas the ferromagnetic thin films were mainly produced by laser ablation,[2,3] or by the sol-gel method,[1]other samples fabricated by precursor deposition,[5] molecular beam epitaxy[6] or powder samples[7] showed no signs of ferromagnetism. In that contradictory situation we propose to study very carefully the magnetic interaction between two nearest neighbor substitutional magnetic ions (Co or Mn) in the dilute limit without any codoping effect. Namely, the numerical values of these exchange couplings are already quite well known by susceptibility[7] or magnetization step measurements[8] which allow a careful check of the LSDA results. Therefore, we present accurate full potential band structure calculations within density functional theory. We find a rather remarkable discrepancy between the measured data and the LSDA results which can be considerably reduced by taking into account more properly the correlation effects of the transition metal ions within the LSDA+U method.

First LSDA studies found ZnO:Co to be ferromagnetic, but ZnO:Mn antiferromagnetic.[4] Pseudopotential calculations on large supercells[9,10] which were performed later on, could specify the different couplings more in detail. They found a competition between ferromagnetic and antiferromagnetic interactions in ZnO:Co[9,10] which we confirm and argued for the necessity of additional electron[9,10] or hole doping[10,12] to stabilize ferromagnetic order. (Such an additional doping will not be studied here.) But the presence of ferromagnetic and antiferromagnetic couplings at the same time would lead to a very small Curie-Weiss constant in contrast to the observed one which is clearly antiferromagnetic.[5,6,7] Even more clear is the contradiction between the measured data and the LSDA results for ZnO:Mn: magnetization step measurements[8] lead to antiferromagnetic exchange integrals of -1.56 and -2.08 meV for the two nearest neighbor positions possible, although the experiment does not allow to assign these values to certain bonds in an unambiguous way. Transforming the energy differences into numerical values of exchange integrals (which was not done in Refs. 9,10) we will show that LSDA overestimates the experimental results considerably. After having stated the discrepancy between LSDA and experiment, we show that the LSDA+U method can cure these deficiencies and leads to reasonable exchange couplings. The importance of the LSDA+U approximation has also recently been pointed out for the related system ZnSe:Mn.[11]

II. SUPERCELL CALCULATIONS

To determine the nearest neighbor exchange couplings we performed several supercell calculations. ZnO crystallizes in the hexagonal wurtzite structure (space group P63mc) with the lattice parameters $a = 3.2427$ Å and $c = 5.1948$ Å.[13] We consider here pure substitutional defects and neglect the influence of lattice relaxations. Due to the wurtzite structure there are two crystallographically different nearest neighbor positions: the in-plane nearest neighbor within the plane perpendicular to the hexagonal axis **c** and the out-of-plane nearest neighbor. Their magnetic couplings were studied by using 4 different supercells (A,B,C, and D). Each supercell is formed by multiples of the primitive lattice vectors **a**, **b**, and **c**, like the $2 \times 2 \times 1$ supercell A, shown in Fig. 1. The

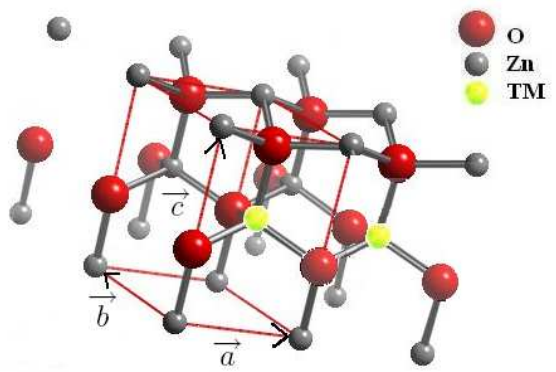

FIG. 1: (Color online) Crystal structure of the supercell A. (TM = Co, Mn)

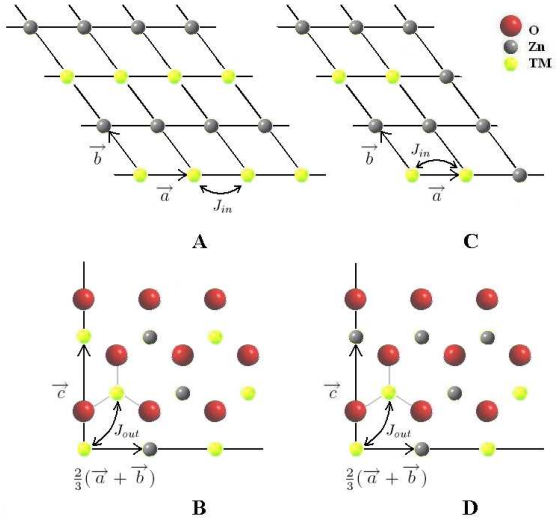

FIG. 2: (Color online) $(\vec{a},\vec{b})$ plane corresponding to supercells A and C as well as $(\frac{2}{3}(\vec{a}+\vec{b}), \vec{c})$ plane corresponding to supercells B and D, with the definition of in-plane and out-of-plane exchange constants J_{in} and J_{out}, respectively. (TM = Co, Mn)

supercells A and C probe the in-plane nearest neighbor exchange J_{in} (see Fig. 2) by a chain of Co (or Mn) impurities (supercell A) or an isolated pair ($3\times2\times1$ supercell C). The out-of-plane exchange J_{out} is probed by the $2\times2\times1$ supercell B (chain) and the $2\times2\times2$ supercell D (pair). The so defined supercells A-D coincide with those used in Ref. 9.

The supercell calculations were performed using the full-potential local-orbital (FPLO) band structure scheme.[14] In the FPLO method a minimum basis approach with optimized local orbitals is employed, which allows for accurate and efficient total energy calculations. For the present calculations we used the following basis set: Zn, Co(Mn) 3*s*3*p*:4*s*4*p*3*d*, O 2*s*2*p*;3*d*. The inclusion of the transition metal 3*s* and 3*p* semicore states into the valence was necessary to account for non-negligible core-core overlap, and the O 3*d* states were used to improve the completeness of the basis set. The site-centered potentials and densities were expanded in spherical harmonic contributions up to $l_{max} = 12$.

The exchange and correlation potential was treated in two different ways. First, the local spin-density approximation (LSDA) was used in the parametrization of Perdew and Wang.[15] However, as will be shown more in detail below, this approximation has severe deficiencies in the present case. The Co(Mn) 3*d* states are in reality more localized than in the LSDA calculation. This correlation effect was taken into account by using the FPLO implementation of the LSDA+U method in the atomic limit scheme.[16,17] The convergence of the total energies with respect to the **k**-space integrations were checked for each of the supercells independently. We found that $8\times8\times8 = 512$ **k**-points were sufficient in all cases, and this parameter was used in the calculations reported below.

III. EXCHANGE COUPLINGS

The Zn^{2+} ion in ZnO has a completely filled 3*d* shell and, correspondingly, no magnetic moment. If Zn is replaced by Co or Mn, the valence 2+ is not changed, which is also proved by our bandstructure results below. It means that these substitutional impurities provide no charge carriers. The configuration of Co^{2+} is d^7 and that of Mn^{2+} is d^5. Therefore, they have a spin $S = 3/2$ or $S = 5/2$, correspondingly. The tetrahedral and trigonal crystal fields, together with the spin-orbit coupling, lead to a magnetic anisotropy. But they are not large enough to destabilize the high-spin states in the given cases, as supported by electron paramagnetic resonance and magnetization measurements (see Refs. 6,18,19 for ZnO:Co and Ref. 20 for ZnO:Mn).

The present work is devoted to determine the dominant exchange couplings between two localized magnetic ions. It can be expected that the dominant couplings occur between nearest neighbor impurities, each carrying a local spin $\mathbf{S}_i$. Then, the Heisenberg Hamiltonian for a localized pair of spins is given by

$$H = -2J\mathbf{S}_i\mathbf{S}_j \ . \qquad (1)$$

The corresponding total energies for ferromagnetic (FM) and antiferromagnetic (AFM) arrangements of the two spins are

$$\begin{aligned} E_{FM} &= -J\left[S_T(S_T+1) - 2S(S+1)\right] \ , \\ E_{AFM} &= J\left[2S(S+1)\right] \ , \end{aligned} \qquad (2)$$

with the total spin $S_T = 2S$ of two parallel spins S. This leads to the energy difference between the FM and AFM states per magnetic ion:

$$\Delta E = \frac{E_{FM} - E_{AFM}}{2} = -\frac{J}{2}S_T(S_T+1) \ , \qquad (3)$$

with $S_T = 3$ or 5 for Co or Mn. That energy difference can be compared with the corresponding energy differences of isolated pairs in the supercells C and D. The supercells A and B, however, correspond to chains of magnetic ions. For our purpose, it is sufficient to use an approximative expression for the energy difference between FM and AFM states of a Heisenberg chain. Then, each magnetic ion has two nearest neighbor magnetic ions which doubles the previous energy difference (3):

$$\Delta E = \frac{E_{FM} - E_{AFM}}{2} = -JS_T(S_T + 1)\,. \qquad (4)$$

That result can also be calculated more explicitly by comparing the energies of the FM and AFM states of a Heisenberg chain decomposed into a series of pairs.

It is remarkable that the so defined exchange couplings are experimentally measurable. They will be denoted here as J_{in} and J_{out} for the in-plane and out-of-plane nearest neighbors, respectively. The most precise measurements had been performed using magnetization steps[8] for the case of ZnO:Mn which leads to different values for J_{in} and J_{out}. We are not aware of such measurements for ZnO:Co. An average value of J_{in} and J_{out} is however accessible by susceptibility measurements.[7]

IV. RESULTS

A. ZnO:Co

The density of states (DOS) of the FM solution (for supercells A and B) is shown in Fig. 3. Its main features agree with previous calculations.[9] The minority and majority Co $3d$ states are found to lie mainly in the gap between the valence band of predominantly oxygen $2p$ character and the Zn $4s$-$4p$ conduction band. The Zn $3d$ states are located at about -7 eV at the bottom of the valence band, deep below the Fermi level. The occupation of the Co $3d$ level is close to $3d^7$ and the magnetization $M_s^{FM}(Co) = 2.6\mu_B$, i.e. rather close to $S = 3/2$. The majority Co $3d$ states are located just above the oxygen valence band. There is a small hybridization of the minority $3d$ level with the conduction band which makes the material half-metallic in the LSDA (see also Refs. 9,10). However, this half-metallic character would correspond to a partial electron doping and is an artifact of the LSDA solution.

Already the gap of pure ZnO (experimental gap: 3.3 eV) is underestimated by LSDA (FPLO leads to a gap of 1.4 eV). To study the $3d$ levels of an isolated Co impurity we calculated the electronic structure of a $CoZn_7O_8$ supercell by LSDA. The corresponding DOS of the FM solution is rather close to that one shown in Fig. 3, but the band structure (not shown) allows a better analysis of the impurity levels, free of hybridization effects between neighboring impurities. For instance, the crystal field splitting of the Co $3d$ levels is clearly visible at the

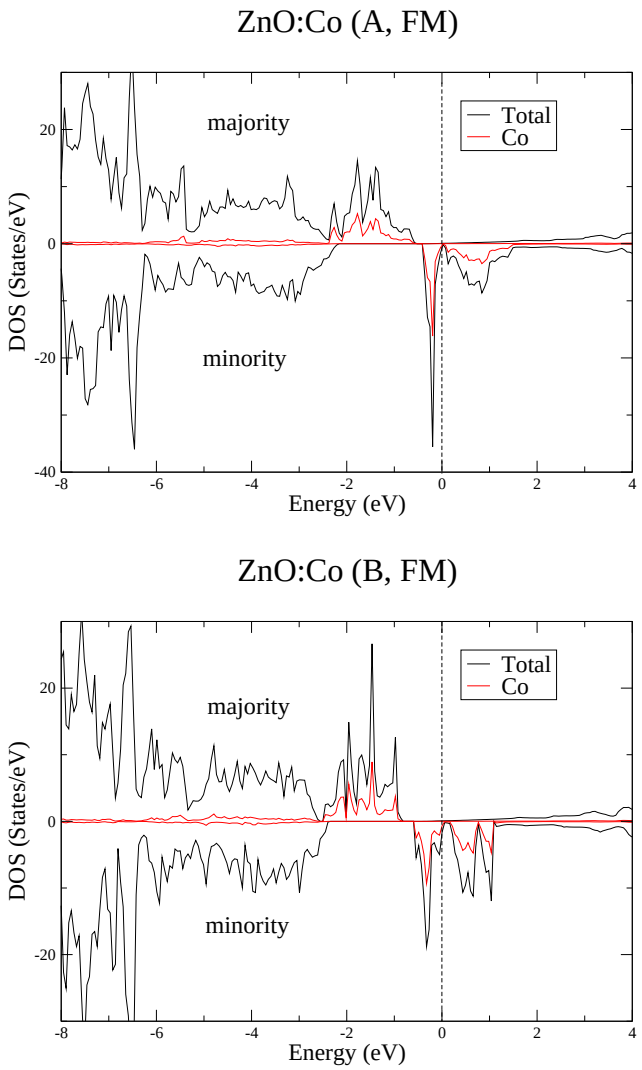

FIG. 3: (Color online) Comparison of total and partial DOS (for 1 Co atom) for supercells A and B, ZnO:Co, in the FM case obtained by LSDA.

Γ-point. In each of the spin channels the two-fold degenerated e_g levels are situated below the t_{2g} orbitals, for majority spin by about 0.5 eV. The e_g levels remain degenerate in the trigonal case, whereas the t_{2g} ones split into a lower singlet and an upper doublet. This trigonal splitting is of the order of 0.2 eV. Due to hybridization effects, the Co $3d$ impurity band is considerably broader in Fig. 3 than for $CoZn_7O_8$ by roughly a factor of three for majority spin. That shows that hybridization and crystal field splitting are of the same order of magnitude for two neighboring Co impurities in ZnO.

The differences of total energies between FM and AFM solutions give the corresponding exchange couplings in the way described above. The values for in-plane and out-of-plane exchange J_{in} and J_{out} are collected in Tables I and II. Like in the previous pseudopotential calculations[9,10] the in-plane exchange is antiferromagnetic, but the out-of-plane exchange ferromagnetic.

Cell	U[eV]	Δ E[meV/Co]	J_{in}[meV]	M_s^{AF}(Co)	M_s^{FM}(Co)
A	0	22	-1.8	2.49	2.60
C	0	16	-2.6	2.54	2.60
A	6	24	-2.0	2.81	2.82
A	8	36	-1.5	2.86	2.86

TABLE I: Calculated in-plane exchange J_{in} for ZnO:Co using LSDA ($U = 0$) and LSDA+U ($F^0 = U \neq 0$, $F^2 = 7.9$ eV and $F^4 = 5.0$ eV) for the supercells A and C. Also given are the corresponding energy differences per Co ion and the magnetic moments.

Cell	U[eV]	Δ E[meV/Co]	J_{out}[meV]	M_s^{AF}(Co)	M_s^{FM}(Co)
B	0	-31	2.6	2.52	2.60
D	0	-14	2.4	2.56	2.60
B	6	12	-1.0	2.81	2.82
B	8	12	-1.0	2.86	2.87

TABLE II: Calculated out-of-plane exchange J_{out} for ZnO:Co using LSDA ($U = 0$) and LSDA+U ($F^0 = U \neq 0$, $F^2 = 7.9$ eV and $F^4 = 5.0$ eV) for the supercells B and D. Also given are the corresponding energy differences per Co ion and the magnetic moments.

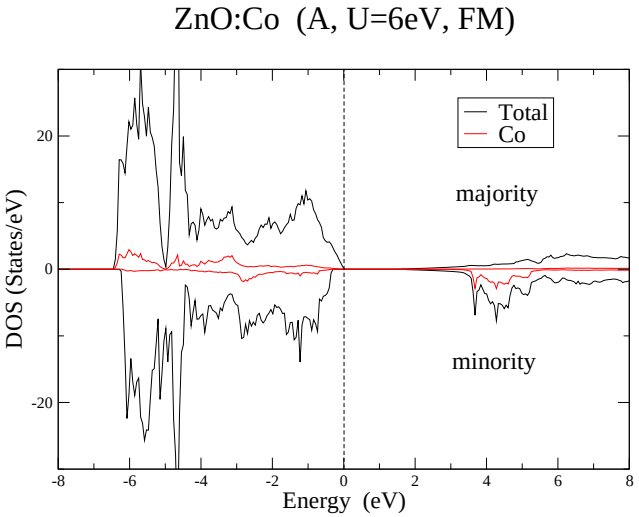

FIG. 4: (Color online) DOS of ZnO:Co, supercell A, in the FM case, calculated with LSDA+U.

The differences between supercells A and C (or between B and D, correspondingly) arise due to finite size effects or deviations from the Heisenberg model. Qualitatively, all available LSDA energy differences agree among each other and with our FPLO results (see Table III). But there are rather remarkable numerical deviations between the different methods. Please note, that the previous authors[9,10] did not convert the LSDA energy differences into exchange couplings. That we have done to allow the comparison with experimental data.

The competition between FM and AFM nearest neighbor exchange in ZnO:Co is in contrast to experimental results[5,6,7] which show dominantly AFM couplings. Other problems of the LSDA solution are the following: (i) the semi-metallic character, (ii) the insufficient localization of the Co 3d states, and (iii) the position of the impurity 3d levels. Namely, photoemission spectroscopy shows them as deep impurity levels close to the valence band.[21] But the experimental energy difference to the top of the valence band of only 0.4 eV is smaller than the corresponding distance of the center of gravity of the Co 3d level (about 1 eV for majority spin).

So, we should look for a theoretical method which takes into account correlation effects more properly. One has to distinguish the correlation in valence and conduction band leading to the incorrect gap value and the correlation effects in the Co 3d orbitals. The first effect might be repaired by the GW approximation,[22] or including the self interaction correction (SIC) as proposed in Ref. 23. But we do not expect that it would considerably improve the exchange couplings. The correlation in the Co 3d shell will be taken into account in our present work by the LSDA+U scheme using the atomic limit functional.[24] We also tried the "around mean field" version of LSDA+U which gives similar results as reported below for ZnO:Co, but which leads to no improvements for ZnO:Mn due to the known peculiarities of this functional for the d^5 configuration.[16,24] The parameters for ZnO:Co have been chosen similar to those for CoO,[17] namely the Slater parameters F^2 and F^4 such that the Hund's rule exchange $J^H = (F^2 + F^4)/14 = 0.92$ eV and the ratio $F^4/F^2 = 0.625$ are close to ionic values[25] which leads to $F^2 = 7.9$ eV and $F^4 = 5.0$ eV. The parameter $F^0 = U$ is less well known since it is more affected by screening effects. We found that a value of at least 3 eV is necessary to stabilize an insulating solution. In the region of realistic F^0 parameters its influence on the values J_{in} and J_{out} is small as indicated by the comparison of results for $F^0 = 6$ and 8 eV in Tables I and II.

The DOS (Fig. 4) shows then clearly an insulating state and the occupied Co levels are much closer to the valence band than in LSDA in better agreement with photoemission data.[21] The gap value ($E_g \approx 0.7$ eV for the FM case, $F^0 = 6$ eV) is not much improved, but that can also not be expected since we did not change the potentials for oxygen or zinc s-p states. However, it is remarkable that now both exchange couplings are antiferromagnetic.

We find the in-plane exchange $J_{in} = -2.0$ meV to be larger than the out-of-plane exchange $J_{out} = -1.0$ meV (for $U = 6$ eV). Experimentally, the antiferromagnetic nearest neighbor exchange was determined to be $J = -33$ K or -2.8 meV from the high-temperature Curie-Weiss constant of the magnetic susceptibility,[7] which exceeds slightly our values.

	J_{in}^{Co}	J_{out}^{Co}	J_{in}^{Mn}	J_{out}^{Mn}
Ref. 9 cells A, B	-2.8	0.1		
Ref. 9 cells C, D	-3.5	0.2		
Ref. 10	-3.3	2.5	-4.0	-3.3

TABLE III: Available theoretical LSDA results for J_{in} and J_{out} (all data in meV) of ZnO:Co and ZnO:Mn taken from the literature. The published energy differences were converted into exchange constants.

B. ZnO:Mn

In Fig. 5, we show the DOS of ZnO:Mn, calculated with supercell A and a ferromagnetic arrangement of the Mn moments. As in the case of ZnO:Co, LSDA yields a metallic solution. The Mn 3*d* shell is approximately half filled and the exchange splitting between the centers of gravity of the occupied majority and unoccupied minority subbands is about 3.5 eV. The total spin moment $4.96\mu_B$/Mn is close to the expected $S = 5/2$ value. The Mn atoms carry a spin moment of about $4.6\mu_B$, but also their four nearest neighbor O atoms have a weak induced spin moment. The Mn 3*d* impurity states are mainly located in the upper part of the ZnO gap and weakly hybridize with the Zn 4*s*-4*p* conduction band, which gives the solution a metallic character. Measurements of the band gap of ZnO:Mn films[26] (see Ref. 27 for an overview) find a slight blue shift of the absorption edge with a significant amount of mid gap absorption above 2.5 eV. This is consistent with a position of the impurity levels around the upper edge of the valence band in contrast to the LSDA result.

As shown in the lower graph of Fig. 5, LSDA+U shifts the highest occupied Mn 3*d* levels to the top of valence band, so that the solution becomes insulating. The parameters used in the calculation are $U = F^0 = 6$ eV, $F^2 = 7.4$ eV and $F^4 = 4.6$ eV, corresponding to $J^H = 0.86$ eV, the value chosen for MnO in Refs. 17,25. As in the case of ZnO:Co, the value of the band gap $E_g \approx 0.4$ eV is smaller than the experimental one (see discussion above), but the position of the Mn 3*d* impurity levels is considerably improved. Compared to the LSDA calculation, the partial Mn 3*d* DOS is slightly broadened and the unoccupied Mn 3*d* minority spin states are shifted further away from the Fermi level. The total spin moment is now $5\mu_B$ corresponding to an ideal $S = 5/2$ situation with the magnetic contributions almost entirely due to Mn (see Tables IV and V).

In contrast to the case of ZnO:Co, LSDA yields an AFM exchange coupling for both types of nearest neighbor pairs in ZnO:Mn. This is in qualitative agreement with the magnetization step measurements of Ref. 8, where values $J_{in} = -2.08$ meV and $J_{out} = -1.56$ meV have been obtained. However, the LSDA values $J_{in} = -4.9$ meV and $J_{out} = -4.1$ meV are 2-3 times larger than the experimental ones. Similar results have also been obtained by Sluiter *et al.*[10], who find both couplings to be strongly AFM (see Tab. III). However, the rather poor quantitative agreement between the calculated and measured J values indicates that the Mn impurity levels are not well described within LSDA. Again, the LSDA+U functional strongly improves the agreement of the calculations with experimental data. Taking $U = 6$ eV, we obtain $J_{in} = -2.0$ meV and $J_{out} = -1.3$ meV, close to the measured values. As can be seen in Tables IV and V, the calculated exchange couplings depend only moderately on the choice of the U-parameter. The larger coupling is obtained for the in-plane pairs despite the larger distance, as was already assumed in Ref. 8.

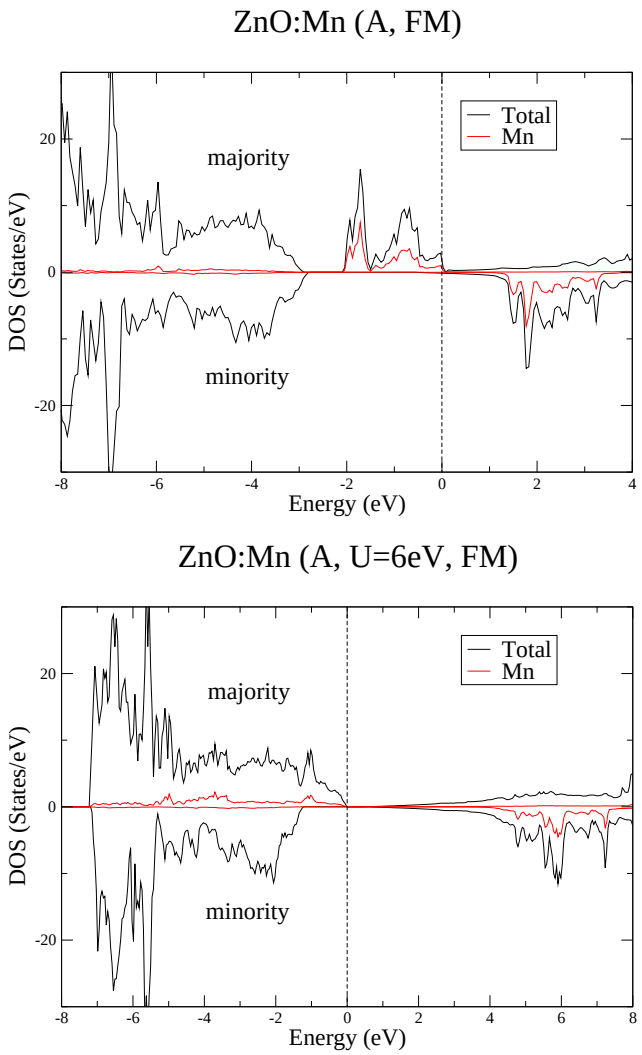

FIG. 5: (Color online) DOS of ZnO:Mn, comparison of LSDA and LSDA+U, supercell A.

V. DISCUSSION

The reason for the competition of FM and AFM exchange couplings within LSDA for ZnO:Co is schematically shown in Fig. 6. Let us first consider an isolated

Cell	U[eV]	Δ E[meV/Mn]	J_{in}[meV]	M_s^{AF}(Mn)	M_s^{FM}(Mn)
A	0	147	-4.9	4.52	4.62
C	0	74	-4.9	4.57	4.62
A	6	59	-2.0	4.87	4.89
A	8	48	-1.6	4.94	4.94

TABLE IV: Calculated in-plane exchange J_{in} for ZnO:Mn using LSDA ($U = 0$) and LSDA+U ($F^0 = U \neq 0$, $F^2 =$ 7.4 eV and $F^4 = 4.6$ eV) for the supercells A and C. Also given are the corresponding energy differences per Mn ion and the magnetic moments.

Cell	U[eV]	Δ E[meV/Mn]	J_{out}[meV]	M_s^{AF}(Mn)	M_s^{FM}(Mn)
B	0	122	-4.1	4.55	4.64
D	0	57	-3.8	4.57	4.61
B	6	40	-1.3	4.88	4.89
B	8	30	-1.0	4.94	4.94

TABLE V: Calculated out-of plane exchange J_{out} for ZnO:Mn using LSDA ($U = 0$) and LSDA+U ($F^0 = U \neq 0$, $F^2 =$ 7.4 eV and $F^4 = 4.6$ eV) for the supercells B and D. Also given are the corresponding energy differences per Mn ion and the magnetic moments.

Co ion in ZnO. The $3d$ levels are split by the crystal field (CF) into lower e_g and upper t_{2g} levels. They are also influenced by the exchange splitting between spin up and spin down electrons caused by the local Hund's rule exchange. These local energy levels are filled with 7 electrons in the case of Co. The LSDA-DOS (Figs. 3,5) shows that the CF splitting is smaller than the exchange splitting. Fig. 6 presents the hybridization effect on the Co $3d$ energy levels if the two Co ions come close together. The hybridization leads to the formation of a pair of bonding and antibonding hybrid orbitals for each $3d$ energy level E_i of Co. The bonding and antibonding orbitals have energies $E_i - \Delta E_i$ and $E_i + \Delta E_i$, correspondingly. Therefore, the complete filling of these two orbitals does not lead to an energy gain, but a partial filling does. In such a way, the energy gain for an AFM arrangement of spins is evident. For a FM arrangement, the energy gain is only possible by a crossing of the e_g and t_{2g} levels for minority spin. This competition between the FM and the AFM energy gain is apparently not identical for in-plane and out-of-plane exchange, leading to different signs of the exchange couplings. However, as already discussed, that is an artifact of the LSDA solution.

In LSDA+U (Fig. 7) the unoccupied minority spin energy levels are much higher than the occupied ones. Therefore, the crossing of minority e_g and t_{2g} energy levels, and also the FM energy gain, is not possible. As a consequence, one finds an AFM superexchange coupling in ZnO:Co independent of the geometrical configuration.

The situation for ZnO:Mn is different. In that case, only the majority spin is completely filled with 5 electrons and the minority spin is nearly empty in LSDA, and completely empty in LSDA+U. Since the exchange

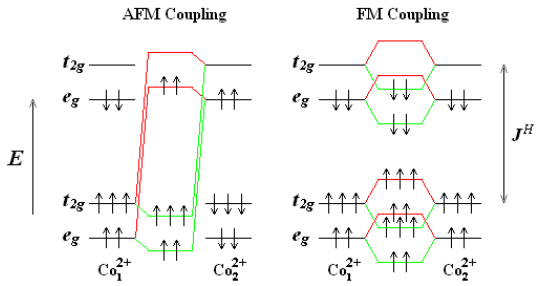

FIG. 6: (Color online) Schematic view of hybridization and CF effects on two close Co $3d$ shells in the LSDA case, comparison between AFM and FM couplings. The energy levels of majority spin are lower in energy than minority spin ones due to the Hund's coupling J^H.

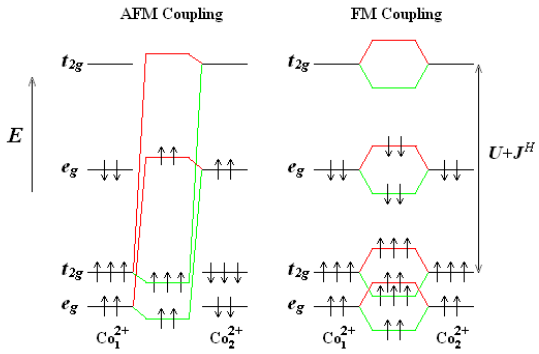

FIG. 7: (Color online) Schematic view of hybridization and CF effects on two close Co $3d$ shells in the LSDA+U case, comparison between AFM and FM couplings. The energy levels of majority spin are lower in energy than minority spin ones due to the Hund's coupling J^H. The occupied energy levels are lower in energy than unoccupied ones due to the $3d$ shell correlation effect U.

splitting is larger than the CF splitting, there is no energy gain possible for a FM arrangement of impurity spins neither in LSDA nor in LSDA+U. The distance between occupied and unoccupied energy levels increases in LSDA+U. Therefore, the energy gain is reduced and leads to exchange couplings which are much closer to the experimental values obtained by magnetization step measurements than those obtained by LSDA. It should be noted that our calculation confirms also the assignment of Ref. 8 that J_{in} corresponds to the largest coupling.

Of course, there are still numerical error sources on the exchange couplings J_{in} and J_{out} which were calculated by LSDA+U. First of all, we should note the poor knowledge of correlation parameters U, F^2, and F^4, which influences the results. Second, there might still be finite size effects due to the specific form of the supercells chosen. And finally, also a small basis set dependence of the FPLO method cannot be excluded. All together, we would estimate an upper error of about ±30 per cent for the calculated exchange couplings.

VI. CONCLUSIONS

In the dilute limit, nearest neighbor pairs of Co and Mn-impurities in ZnO have antiferromagnetic exchange couplings. That is the result of theoretical calculations which take into account the electron correlations in the impurity 3*d* shell properly, and is in agreement with the experimental results. This AFM nearest neighbor exchange excludes ferromagnetism for pure substitutional Co or Mn defects in ZnO in the dilute limit. The observed FM in ZnO:Co and ZnO:Mn should have a different origin. There are several proposals in the literature like secondary phases[28] or cation vacancies or other defects.[29,30]

The LSDA predictions might be misleading and should be considered with care since they do not correctly take into account the localized character of the transition metal impurities. On the contrary, the LSDA+U values are in good agreement with experimental exchange constants derived from magnetization step measurements and high-temperature susceptibility data.[7,8] So our study puts considerable doubts on the value of pure LSDA predictions (as published for instance in Refs. 3,10), at least in the case without additional electron or hole doping.

VII. ACKNOWLEDGEMENTS

We thank Laurent Raymond and Ulrike Nitzsche for help with the numerical calculations and the NATO science division grant (grant CLG 98 1255) for financial support. We thank also Anatoli Stepanov, Pascal Sati and Roman Kuzian for useful discussions.

[1] H.J. Lee, S.-Y. Jeong, C. R. Cho and C. H. Park, Appl. Phys. Lett. **81**, 4020 (2002).
[2] W. Prellier, A. Fouchet, B. Mercey, C. Simon and B. Raveau, Appl. Phys. Lett. **82**, 3490 (2003).
[3] P. Sharma, A. Gupta, K.V. Rao, F.J. Owens, R. Sharma, R. Ahuja, J.M.O. Guillen, B. Johansson, and G.A. Gehring, Nat. Mater. **2**, 673 (2003).
[4] K. Sato and H. Katayama-Yoshida, Physica E **10**, 251 (2001).
[5] G. Lawes, A. S. Risbud, A. P. Ramirez and R. Seshadri, Phys. Rev. B **71**, 045201 (2005).
[6] P. Sati, R. Hayn, R. Kuzian, S. Regnier, S. Schäfer, A. Stepanov, C. Morhain, C. Depars, M. Laügt, M. Goiran and Z. Golacki (unpublished).
[7] S.W. Yoon, S.-B. Cho, S.C. We, S. Yoon, B.W. Suh, H.K. Song, and Y.J. Shin, Journal of Applied Physics **93**, 7879 (2003).
[8] X. Gratens, V. Bindilatti, N.F. Oliveira, Y. Shapira, S. Foner, Z. Golacki, and T.E. Haas, Phys. Rev. B **69**, 125209 (2004).
[9] E.C. Lee and K. J. Chang, Phys. Rev. B **69**, 085205 (2004).
[10] M.H.F. Sluiter, Y. Kawazoe, P. Sharma, A. Inoue, A.R.Raju, C. Rout, and U.V. Waghmare, Phys. Rev. Lett. **94**, 187204 (2005).
[11] L. M. Sandratskii, Phys. Rev. B **68**, 224432 (2003).
[12] N.A. Spaldin, Phys. Rev. B **69**, 125 201 (2004).
[13] T.M. Sabine and S. Hogg, Acta Cryst. B **25**, 2254 (1969).
[14] K. Koepernik and H. Eschrig, Phys. Rev. B **59**, 1743 (1999).
[15] J.P. Perdew and Y. Wang, Phys. Rev. B **45**, 13244 (1992).
[16] H. Eschrig, K. Koepernik, and I. Chaplygin, J. Solid State Chem. **176**, 482 (2003).
[17] V.I. Anisimov, J. Zaanen, and O.K. Andersen, Phys. Rev. B **44**, 943 (1991).
[18] T. Estle and M. De Wit, Bull. Am. Phys. Soc. **6**, 445 (1961).
[19] N. Jedrecy, H.J. von Bardeleben, Y. Zheng, and J.-L. Cantin, Phys. Rev. B **69**, 041308(R) (2004).
[20] J. Schneider and S. R. Sircar, Z. Naturforschg. **17a**, 570 (1962).
[21] S. C. Wi, J.-S. Kang, J. H. Kim, S.-B. Cho, B. J. Kim, S. Yoon, B. J. Suh, S. W. Han, K. H. Kim, K. J. Kim, B. S. Kim, H. J. Song, H. J. Shin, J. H. Shim and B. I. Min, cond-mat, 0307524 (2003).
[22] M. S. Hybertsen and S. G. Louie, Phys. Rev. Lett. **55**, 1418 (1985).
[23] A. Filippetti and N. A. Spaldin, Phys. Rev. B **67**, 125109 (2003).
[24] M. T. Czyzyk and G. A. Sawatzky, Phys. Rev. B **49**, 14211 (1994).
[25] V. I. Anisimov, I. V. Solovyev, M. A. Korotin, M. T. Czyzyk and G. A. Sawatzky, Phys. Rev. B **48**, 16929 (1993).
[26] X. M. Cheng and C. L. Chien, J. Appl. Phys. **93**, 7876 (2003).
[27] Ü. Özgür, Ya. I. Alivov, C. Liu, A. Teke, M. A. Reshchikov, S. Dogan, V. Avrutin, S.-J. Cho, and H. Morkoc, J. Appl. Phys. **98**, 041301 (2005).
[28] M. A. Garcìa, M. L. Ruiz-González, A. Quesada, J. L. Costa-Kramer, J. F. Fernández, S. J. Khatib, A. Wennberg, A. C. Caballero, M. S. Martín-González, M. Villegas, F. Briones, J. M. González-Calbet and A. Hernando, Phys. Rev. Lett. **94**, 217206 (2005).
[29] M. Venkatesan, C. B. Fitzgerald, J. G. Lunney and J. M. D. Coey, Phys. Rev. Lett. **93**, 177206 (2004).
[30] C. H. Park and D. J. Chadi, Phys. Rev. Lett. **94**, 127204 (2005).